

Infrared spectra of the one-dimensional quarter-filled Wigner lattice compounds δ -(EDT-TTF-CONMe₂)₂X (X = AsF₆, Br): Domain-wall excitations

Ágnes Antal,^{1,2} Tobias Knoblauch,¹ Martin Dressel,¹ Patrick Batail,³ and Natalia Drichko^{1,4}

¹*Physikalisches Institut, Universität Stuttgart, Pfaffenwaldring 57, 70550 Stuttgart, Germany*

²*Institute of Physics, Budapest University of Technology and Economics, and Condensed Matter Research Group of the Hungarian Academy of Sciences, P.O. Box 91, H-1521 Budapest, Hungary*

³*Laboratoire CIMMA, UMR 6200 CNRS-Université d'Angers, Bt. K, UFR Sciences, 2 Boulevard Lavoisier, F-49045 Angers, France*

⁴*Department of Physics and Astronomy, Johns Hopkins University, Baltimore, Maryland, USA*

(Received 23 November 2012; revised manuscript received 5 January 2013; published 13 February 2013)

Optical investigations of quarter-filled charge ordered insulators δ -(EDT-TTF-CONMe₂)₂X, X = AsF₆, Br are reported. The spectra evidence the one-dimensional nature of the systems at all temperatures. The charge order exists already at room temperature, the optical gap is estimated to be of the order of 550 cm⁻¹ for the X = Br compound and about 700 cm⁻¹ for the X = AsF₆ material. The optical response in the direction of the stacks is discussed in terms of domain-wall excitations of one-dimensional quarter-filled Wigner lattice at moderate values of nearest-neighbor electronic repulsion. A similarity between the effects of temperature contraction and chemical pressure is found.

DOI: [10.1103/PhysRevB.87.075118](https://doi.org/10.1103/PhysRevB.87.075118)

PACS number(s): 71.20.Rv, 72.20.-i, 72.15.Nj, 87.50.wp

I. INTRODUCTION

One of the experimental realizations of a Wigner crystal is a charge-ordered insulator with a large difference between charges on crystallographically equivalent sites. In contrast to charge density wave, which is a charge modulation that occurs due to nesting of quasi-one-dimensional (quasi-1D) Fermi surface, Wigner crystal is a “real-space” effect, which originates in high electronic repulsion. The realization of a Wigner crystal in actual materials is scarce, since quasi-one-dimensional crystals tend to structural instabilities.

In this paper, we present a study of infrared frequency-dependent conductivity of quarter-filled quasi-1D charge-ordered insulators δ -(EDT-TTF-CONMe₂)₂X, X = Br, AsF₆ (further on EDT₂-Br and EDT₂-AsF₆) at temperatures between 300 and 10 K. In these materials, the conductance band is formed by overlapping π orbitals of the EDT-TTF-CONMe₂ molecular lattice sites within stacks of the EDT-TTF-CONMe₂ molecules. By stoichiometry, each EDT-TTF-CONMe₂ lattice site carries +0.5e charge. The real distribution of charge in the quasi-1D stacks is different: charge disproportionation between the neighboring molecular lattice sites EDT-TTF-CONMe₂ is 1 : 9 (see Refs. 1–3). This $4k_f$ modulated charge ordered state is present already at room temperature due to the relatively small size of transfer integrals between the molecules (narrow bands) and explains the insulating behavior found in both compounds.^{1–3} The charge order pattern is displayed in the insert in Fig. 1. EDT₂-Br and EDT₂-AsF₆ do not show dimerization in the chains in the whole measured temperature range. Thus they are the “family” of quasi-1D organic conductors that maintains quarter filling of the conductance band down to the lowest temperatures.⁴ They also retain their quasi-1D properties and do not show a dimensional crossover on cooling as TMTTF and TMTSF based materials (see, for example, Refs. 5 and 6).

Similarly to the Berchgaard salts, in the δ -(EDT-TTF-CONMe₂)₂X family, the hydrostatic pressure can control a ground state. The pressure-temperature phase diagram of

δ -(EDT-TTF-CONMe₂)₂X based on NMR and transport results was described by Auban-Senzier *et al.*³ Changing the size of the anion molecules by altering their chemical composition leads to effects similar to the application of hydrostatic pressure.³ It was shown that changing the AsF₆ anion to Br leads to a similar effect as applying 7 kbar of hydrostatic pressure, moving the compound closer to the metallic state. The EDT₂-Br crystal is a better conductor at room temperature by more than two orders of magnitude.³ The room temperature conductivity for EDT₂-AsF₆ was reported to be around 0.003 $\Omega^{-1}\text{cm}^{-1}$, while for EDT-Br it is 0.1 $\Omega^{-1}\text{cm}^{-1}$.

The main electronic parameters to describe the ground state of quarter-filled 1D materials are transfer integrals t between the EDT-TTF-CONMe₂ molecular lattice sites in quasi-1D chains, and the high on-site (U) and nearest-neighbor (V) electron-electron repulsions. The relative simplicity of the electronic structure makes these materials good model systems to compare to theoretical results on one-dimensional quarter-filled systems with strong electronic correlations. And indeed, our experimental optical results are in a good agreement with a model of domain wall excitations proposed for 1D Wigner crystals.^{7,8}

Presented in this work optical conductivity spectra in the range of 600–7000 cm⁻¹ show an intense wide maximum in the mid-infrared range only along 1D stacks of EDT-TTF-CONMe₂ molecules, and low conductivity with no frequency dependence in the two perpendicular to the stacks polarizations, being a direct evidence of 1D electronic structure. On cooling, we observe the large shift of the mid-infrared maximum in the optical conductivity to lower frequencies, which correlates with the decrease of the lattice parameter in the stacks direction. The comparison of EDT₂-Br and EDT₂-AsF₆ spectra at different temperatures demonstrates a similarity between the effects of “chemical pressure” and the pressure due to thermal contraction. The exceptionally strong effect of both temperature and “chemical pressure” on the position of the mid-infrared maximum in conductivity spectra, which was never observed in quasi-1D organic conductors

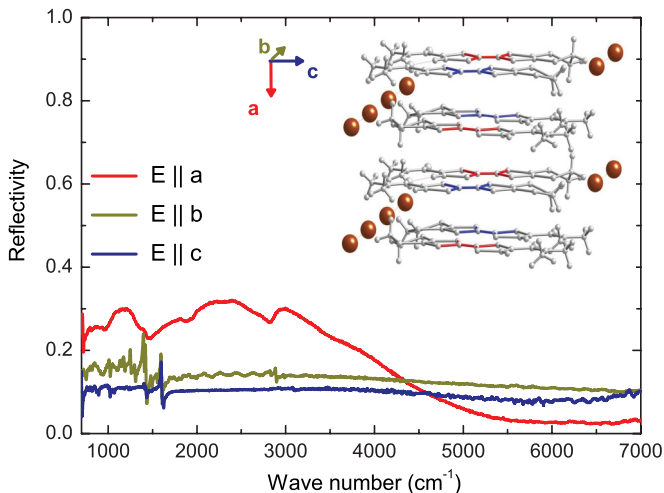


FIG. 1. (Color online) Room-temperature reflectivity spectra of δ -(EDT-TTF-CONMe₂)₂AsF₆ in the three principal directions. The insert shows crystal structure EDT₂-X² with crystal axes (*a*, *b*, *c*) marked. Spheres represent AsF₆ or Br anions. Charge rich and charge poor EDT-TTF-CONMe₂ molecules alternate within the stacks, they are represented by blue and red, respectively. The strongest overlap and the highest reflectivity are observed in the *a* direction, while spectra parallel to *b* and *c* are typical for an insulator.

with structural and Fermi-surface instabilities, suggests the interpretation of the observed spectra in terms of the domain walls excitations in a Wigner crystal.

II. EXPERIMENTAL

Needlelike single crystals of δ -(EDT-TTF-CONMe₂)₂X, X = AsF₆, Br used in our experiments were grown by the method described in Refs. 2 and 4. The crystal structure consists of equidistant stacks of EDT-TTF-CONMe₂ molecules and stacks of anion (X = AsF₆, Br) formed along the *a* crystallographic direction (see Fig. 1). The stacks of EDT-TTF-CONMe₂ are located next to each other along the *b* and are separated by an anion stacks in the *c* direction.

At room temperature, the crystal structure for both compounds is orthorhombic (space group *Pnma*). At 190 K, there is an orthorhombic to monoclinic (*P2₁/a*) phase transition, which is accompanied by twinning. It is a second-order phase transition with a crystallographic angle γ being an order parameter.² Below ~ 10 K both compounds order antiferromagnetically.³ The latter transition occurs at temperatures below those reached in the current experiment.

The calculated transfer integrals between neighboring EDT-TTF-CONMe₂ molecules are highly anisotropic along and perpendicular to the stacks, suggesting 1D electronic structure. The published values are $t_{\parallel} = 71$ meV, $t_{\perp} = -25$ meV for EDT₂-AsF₆ at 300 K,⁴ and $t_{\parallel} = 87$ meV, $t_{\perp} = -32$ meV for EDT₂-Br at 150 K.²

Polarized reflectivity measurements of single crystals of δ -(EDT-TTF-CONMe₂)₂X, X = AsF₆, Br in the 600–7000 cm⁻¹ spectral range were performed using Bruker IFS 66v spectrometer equipped with a microscope. Samples were oriented at room temperature by IR polarization measurements with the accuracy of $\pm 2^{\circ}$. The principle optical axes are found

to be parallel to the crystallographic axes and, respectively, to the sides of the crystals. The absolute values of reflectivity were received by visually choosing a mirrorlike part of a naturally grown surface for a measurement and by a comparison of the sample reflectivity with that of an aluminium mirror.

The probing beam was about 50 μ m in diameter, which allowed us to perform the measurements on these small crystals. The largest dimension of the crystals is observed in the *a*-axis direction (around 1 mm); along *b*-axis direction the crystals are of about 0.1 mm, and along *c*-axis direction, they are about 0.05 mm in size. Due to these small sizes of the crystals and low reflectivity values, the temperature dependent measurements were performed only for the (*ab*) surface in case of EDT₂-Br. For the same reasons, at low reflectivity in the low-frequencies region for EDT₂-AsF₆ crystals, we observe low signal to noise ratio and oscillations of reflectivity, but we nevertheless were able to analyze the data, while an error bar of conductivity at lower frequencies and higher temperatures is high.

For measurements at temperatures between 300 and 10 K, the sample was placed on a cold finger of Cryovac microcryostat. To ensure a good temperature contact, the sample was fixed on the sample holder with silver paint.

The conductivity spectra of both compounds were calculated by Kramers-Kronig transformation. The reflectivity was extrapolated by a constant to low frequencies, since the compounds are insulating. A standard high-frequency extrapolation, $R(\omega) \sim \omega^{-2}$ was used.

III. RESULTS

A. Reflectivity

Reflectivity in the 600–7000 cm⁻¹ frequency range was studied in the directions of all three crystal axes for EDT₂-AsF₆ (see Figs. 1 and 2) and in *E* || *a* and *E* || *b* directions for EDT₂-Br (see Fig. 3).

The information on the localized carriers in the 1/4-filled band is received from the analysis of the spectra in *E* || *a*

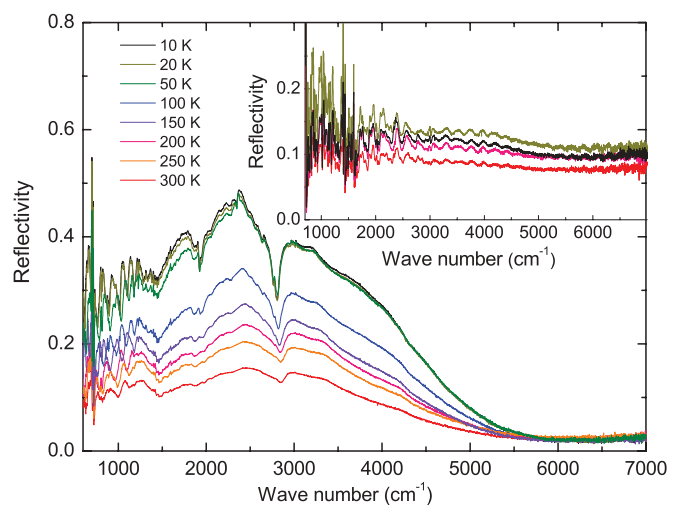


FIG. 2. (Color online) δ -(EDT-TTF-CONMe₂)₂AsF₆ temperature-dependent reflectivity in the *E* || *a* direction and selected temperatures for *E* || *b* (insert).

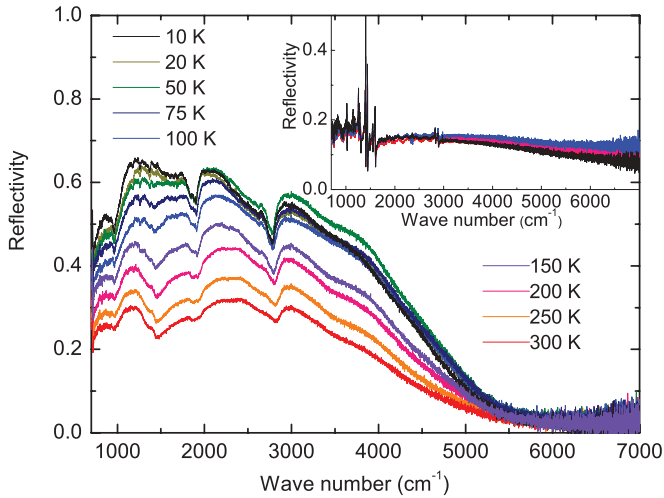


FIG. 3. (Color online) δ -(EDT-TTF-CONMe₂)₂Br temperature-dependent reflectivity in the $\mathbf{E} \parallel \mathbf{a}$ direction and selected temperatures for $\mathbf{E} \parallel \mathbf{b}$ (insert).

direction (parallel to the stacks) and the comparison of those between the studied two systems. At every temperature, the reflectivity in $\mathbf{E} \parallel \mathbf{a}$ polarization of EDT₂-Br is higher than that for the EDT₂-AsF₆ in agreement with the dc measurements showing that EDT₂-Br is a better conductor.

The spectra in the directions perpendicular to the stacks $\mathbf{E} \parallel \mathbf{b}$ and $\mathbf{E} \parallel \mathbf{c}$ are characteristic for insulating behavior, with very low reflectivity independent of frequency but for the sharp features of cation molecular vibrations. Measurements in these directions confirm the 1D electronic structure and the absence of a dimensional crossover on cooling. The details of the temperature dependence of the vibrational features observed in the polarizations perpendicular to the stacks will be discussed separately.⁹

B. Conductivity for polarization parallel to the 1D stacks ($\mathbf{E} \parallel \mathbf{a}$)

The conductivity spectra of EDT₂-AsF₆ and EDT₂-Br calculated from the $\mathbf{E} \parallel \mathbf{a}$ experimental reflectivity by a Kramers-Kronig transformation are presented in Figs. 4 and 5, respectively. The main contribution to the spectra is an asymmetrical wide maximum of apparently electronic origin in the mid-infrared range. This wide maximum shows some fine structure at about 2830, 1890, 1400, and 950 cm⁻¹. The shape of these features changes as the electronic band shifts to lower frequencies with decreasing temperature. Features of this type are typically observed in the spectra of organic compounds due to a coupling of electronic transitions to vibrations of the molecules forming the conducting stacks (EMV coupling).¹⁰

To distinguish between the electronic and vibrational contributions to the spectra we perform a fit of both reflectivity and conductivity spectra to a Lorentz model,¹¹ while describing the features with the Fano formula:^{12,13}

$$\sigma(\omega) = \frac{\Omega_p^2}{4\pi} \frac{\omega}{i(\Omega_0^2 - \omega^2) + \omega\Gamma} + i\sigma_0 \frac{(q - i)^2}{(i + \frac{\omega^2 - \omega_T^2}{\gamma\omega})}. \quad (1)$$

Here, Ω_0 , Ω_p , and Γ are the position, intensity, and width of the electronic maximum, respectively. Parameters of Fano

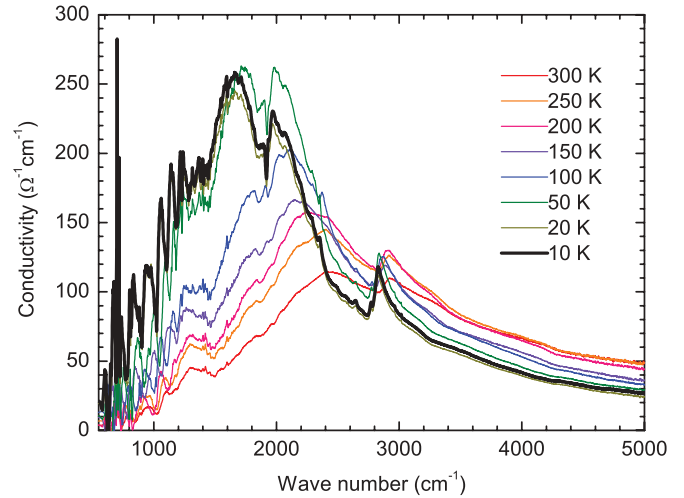


FIG. 4. (Color online) δ -(EDT-TTF-CONMe₂)₂AsF₆ temperature-dependent conductivity in the \mathbf{a} direction.

feature are σ_0 is the conductivity background, ω_T is position, γ is width, and q is a parameter, which characterizes the position of the feature relatively to the electronic transition which activates it. When the positions of an electronic maximum and a vibrational feature coincide, $q = 0$ and a vibrational feature has an antiresonance shape. When these two frequencies move away from each other, q becomes positive or negative, and the shape of a vibrational feature becomes an asymmetric maximum.

An example of the fitting curves is shown in the insert in Fig. 6. The positions of the electronic maxima depending on temperature received from the fit are presented in Fig. 7, while the resulting vibrational frequencies are presented in Table I. On lowering the temperature, the electronic maximum considerably shifts down in frequency in the spectra of both materials (see Figs. 4 and 5 for EDT₂-AsF₆ and EDT₂-Br, respectively). The maximum in the spectra of EDT₂-AsF₆ below 100 K follows exactly the position and intensity of the maximum in the EDT₂-Br at higher temperatures. In Fig. 6, a comparison of the spectra of EDT₂-AsF₆ at 100 K and

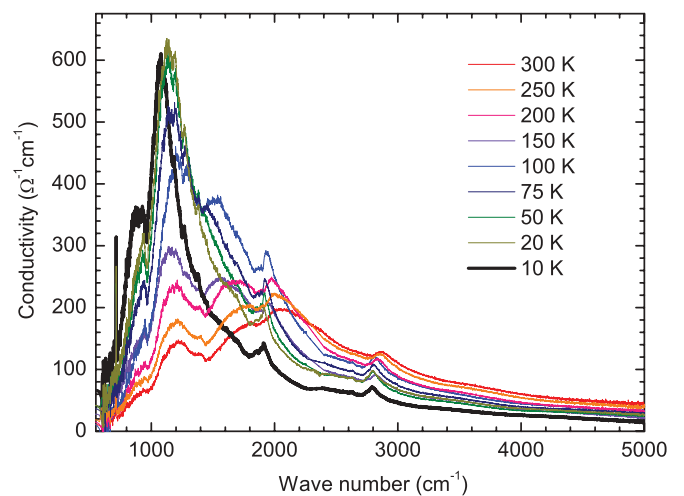


FIG. 5. (Color online) δ -(EDT-TTF-CONMe₂)₂Br temperature-dependent conductivity in the \mathbf{a} direction.

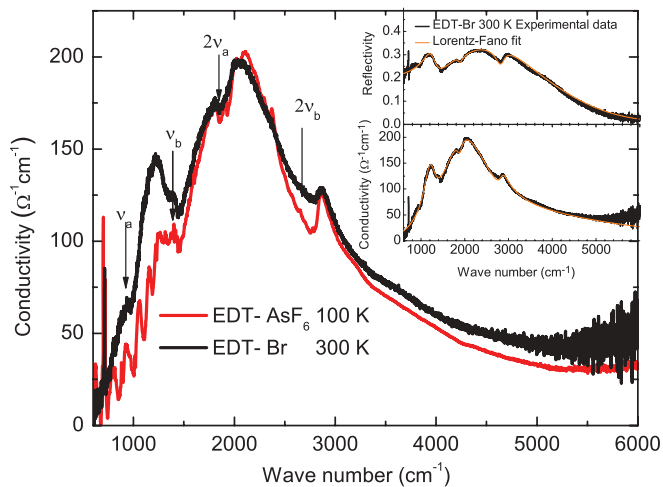


FIG. 6. (Color online) The plot compares conductivity spectra of δ -(EDT-TTF-CONMe₂)₂Br at 300 K and δ -(EDT-TTF-CONMe₂)₂AsF₆ at 100 K. The insert shows an example of a fit of δ -(EDT-TTF-CONMe₂)₂Br spectra at 300 K to Lorentz-Fano formula. The fit is made simultaneously for reflectivity and conductivity.

EDT₂-Br at 300 K shows that the electronic responses are basically equal. The small difference between the two spectra are due to the narrowing of vibrational and electronic features at 100 K compared to 300 K.

The vibrational structure of the electronic maximum is similar for the two studied compounds. The vibrational features change in shape from an antiresonance when their position is close to the electronic maximum to an asymmetric “Fano” shape and finally to a symmetric maximum shape for the higher-frequency features at low temperatures, when the electronic maximum is shifted to much lower frequencies (bands at 1910 and 2870 cm⁻¹ for EDT₂-Br at 10 K).

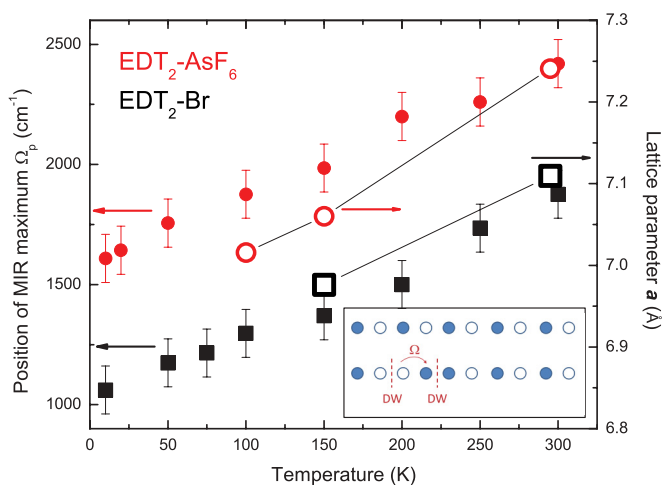


FIG. 7. (Color online) Dependence of the position of the electronic band for δ -(EDT-TTF-CONMe₂)₂Br (black squares) and δ -(EDT-TTF-CONMe₂)₂AsF₆ (red circles) on temperature, received from the Fano-Lorentz fit, compared to the temperature variation of the lattice parameter a .² The insert shows a schematic view of an optical excitation from a charge-rich to a charge-poor site, which leads to a creation of two domain walls in a charge-ordered chain.

TABLE I. Assignment⁹ of the EMV coupled modes in the spectra of EDT₂-Br and EDT-AsF₆, the exact positions are received from the Lorentz-Fano fit.

T K	ν_a cm ⁻¹	$2\nu_a$ cm ⁻¹	ν_a Calc cm ⁻¹	ν_b cm ⁻¹	$2\nu_b$ cm ⁻¹	ν_b Calc cm ⁻¹
100	965	1910	ν_{38} , 992/1048 S-C-S str	1370	2780	ν_{14} , 1533/1545 C=C stretch
300	970	1970		1384	2814	

We find two normal vibrational modes of EDT-TTF-CONMe₂ molecule that show large coupling with the electronic feature and appear in the spectra. Those are central C=C stretching vibration, which typically has large coupling constants in TTF-based molecules,¹⁰ with the unperturbed frequency at 1560 cm⁻¹, and a S-C-S stretch at around 1000 cm⁻¹ (see Ref. 9). The other two features we assign to the overtones of these two modes. Indeed, Ref. 14 shows that the coupling of overtones of certain modes to the electronic transition increases considerably in the charge-ordered state due to the anharmonic vibrational potential.

IV. DISCUSSION: ELECTRONIC RESPONSE

A. 1D electronic structure

Our optical study is a direct proof of the quasi-1D electronic structure of these compounds, see Fig. 1. In particular, the measurements for EDT₂-AsF₆ in $\mathbf{E} \parallel \mathbf{b}$ and $\mathbf{E} \parallel \mathbf{c}$ polarizations show no temperature changes in the spectra in the whole measured temperature range, confirming the 1D behavior.

B. Electronic features: CO band

Summarizing the results, the main feature of the spectra of both compounds in the $\mathbf{E} \parallel \mathbf{a}$ direction is a wide maximum in the mid-infrared region. It considerably shifts to low frequencies on cooling. The maximum has an electronic origin, while the “fine” structure of it is determined by its coupling to vibrations of the EDT-TTF-CONMe₂ molecules.

From the low-frequency edge of the conductivity, we can estimate the optical gap due to charge order to be of about 550 cm⁻¹ for the Br compound and about 700 cm⁻¹ for the AsF₆ material. This is in agreement with the previous studies: in ¹³C NMR³ measurements, it was demonstrated that the charge disproportionation does not change below 200 K, suggesting this value to be the lower estimate for the gap. Previous transport measurements suggested an even higher gap value of 1350 K (~ 940 cm⁻¹) in the case of the AsF₆ compound.⁴

Now we again address Fig. 7, where the positions of the electronic maxima for EDT₂-Br and EDT₂-AsF₆ are plotted against the temperature. The low-frequency shift of the maximum on cooling correlates with the decrease² of the unit cell parameter a due to temperature contraction, the same process would occur on an application of the hydrostatic pressure. The correspondence between pressure and temperature contraction effects is illustrated by the same shape of the spectra of EDT₂-AsF₆ at 100 K and EDT₂-Br at room temperature (see

Fig. 6). Indeed, the values of the lattice parameter a for EDT₂-AsF₆ at 100 K and EDT₂-Br at 300 K are also very close.

The lattice parameter a defines the values of the transfer integrals t between molecules in the 1D stacks, and reflects the increase of the bandwidth due to temperature contraction. An observed shift of the spectral weight to lower frequencies due to the increase of the bandwidth (and thus a decrease of correlation effects) on application of pressure or temperature contraction is intuitively clear, but a model which can describe these effects is necessary.

In a simple model of a charge-ordered system,¹⁵ where a primitive electronic excitation is a charge transfer transition between a charge-rich and a charge-poor sites, a respective band in conductivity spectra would have a maximum at the value of the nearest-neighbor repulsion energy V . A change of its position due to temperature contraction is expected only to the extent to which the decrease of the overlap changes the nearest-neighbor electron repulsion V . It is worth noting, that the strong temperature dependence of the electronic maximum is not typical in the spectra of 1D compounds, for instance, it is not observed for TMTTF salts.

Another approach is a model proposed for 1D Wigner lattice,⁷ where the primitive optical excitations are described as a creation of a pair of interacting domain walls (DW). For the materials studied in this work, this excitation is a charge transfer between a charge-rich and charge-poor lattice sites (see an insert in Fig. 7). A similar model is discussed by Fratini *et al.*⁸ where the authors emphasize the relevance of their study to the spectral properties of quarter-filled nondimerized charge ordered organic conductors IR spectra of which are presented in Ref. 16. Both Mayr *et al.*⁷ and Fratini *et al.*⁸ come to the same conclusions, but Mayr *et al.*⁷ regards a model with lower values of electron repulsion, which is more relevant to our experimental data.

Mayr *et al.*⁷ calculate the optical conductivity spectra of the DW excitations as a function of t/V and temperature. A predicted optical response of DW consists of an asymmetric wide continuum, similar to the experimental spectra observed by us. An important point is that the position of the continuum is sensitive to the t/V value, which would agree with the tendency observed in our experimental data: the maximum shifts from about 0.4 V to 0.2 V , when t/V parameter varies from extremely low values to about 0.1. A typical value of the nearest-neighbor interaction V in TTF-molecule-based materials has a high limit of 0.5 eV (see, e.g., Ref. 17), thus the wide band that we observe in the spectra lies within the frequency range expected by the DW model. For very high values of electronic correlations (small t/V), a narrow sharp excitonic band is predicted to appear on the low-frequency side of the continuum band.^{7,8} We do not observe this excitonic feature, which according to the model gives a low limit on the t/V values observed in the studied systems.

In our case, an increase of t/V occurs due to temperature contraction of the crystal or as an effect of “chemical pressure.” We can estimate if the changes of the observed spectra on cooling agree with the calculated shift of the optical response of DW to low frequencies on the increase of t/V . While we do not have the values of transfer integrals calculated for all compounds and temperatures measured, it is known² that for EDT₂-AsF₆ at 300 K $t_{\parallel} = 0.071$ eV, while the maximum

is observed at $\Omega_p = 2400$ cm⁻¹. The relevant values for EDT₂-Br at 150 K are $t_{\parallel} = 0.087$ eV and $\Omega_p = 1400$ cm⁻¹. We can compare this dependence of frequency of the maximum on t/V , assuming constant V , to the one proposed for DW excitations (see Fig. 7 of Ref. 7). The overall tendency is the same in our experimental data and calculations: the maximum shifts to higher frequencies on the decrease of t/V parameter. Quantitatively we see some discrepancy with the DW model. Within the calculations in the “Wigner lattice” regime, an increase of the frequency of the continuum by 50% implies decrease in t/V by approximately two times. In our spectra, we observe this change of frequency when the t value decreases by about 20%. This discrepancy might mean that the change in the values of inter-site repulsion V is substantial, when it increases on “shrinking” of the crystal. Also, the calculations might underestimate the changes in the spectra that occur with decrease of t .

In contrast to the considerable effect of the temperature contraction, pure temperature effects on the shape and position on the DW excitations are very weak. A small difference between the shape of the spectra of EDT₂-Br at 300 K and EDT₂-AsF₆ at 100 K (see Fig. 6), where the latter shows a narrower mid-infrared (MIR) maximum gives an idea of the subtlety of the temperature effects. Indeed, the theory⁷ also predicts that any considerable change would be observed at temperatures of the order of 0.1 V , which would be above 500 K for the values of V relevant to the EDT₂-Br and EDT-AsF₆.

An increase of the total spectral weight with t/V received from the sum rules is expected.⁷ Indeed, we observe the increase of the spectral weight of the electronic band as it moves to lower frequencies. The insert in Fig. 8 shows a dependence of the spectral weight on the position of the maximum (both depend on t/V for both compounds). The plot demonstrates that the data for both compounds fall on the same dependence. An inconsistency for low temperatures

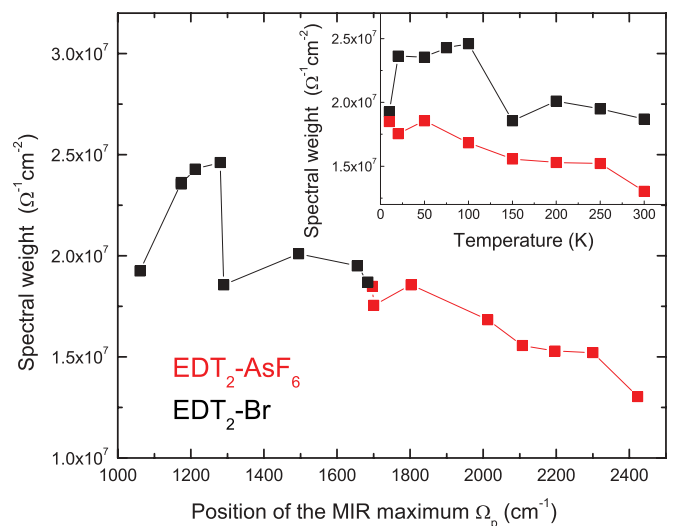


FIG. 8. (Color online) Dependence of the spectral weight of the electronic band for δ -(EDT-TTF-CONMe₂)₂Br and δ -(EDT-TTF-CONMe₂)₂AsF₆ on the position of the maximum, showing that both compounds follow the same dependence. The insert shows the dependence of the spectral weight on temperature for both compounds.

(very low values of the position of the electronic maximum) for EDT₂-Br can be due to the fact that it is already on the edge of Wigner lattice regime or to a larger experimental noise at low frequencies due to the crystal size.

Interestingly, while the shape of the electronic spectra observed for EDT₂-Br and EDT₂-AsF₆ are typical for insulating quasi-1D organic conductors, such a large change of a position of the MIR maximum within insulating state and without closing of the optical gap seems to be unique. For example, conductivity spectra in stacks direction in (TMTTF)₂X¹⁸ under hydrostatic pressure show an appearance of spectral weight at about 1000 cm⁻¹, while the higher frequency maximum observed at ambient conditions at about 2000 cm⁻¹ stays unchanged.

Important differences between the TMTTF-based compounds and EDT₂-X are that the latter materials show (i) an absence of dimerization in the stacks and (ii) a weaker coupling between the stacks. Thus the studied compounds EDT₂-Br and EDT₂-AsF₆ behave as 1D Wigner lattice systems, and as an optical response, we observe excitations of domain walls on a Wigner lattice, while in TMTTF and TMTSF-based materials, the optical response is controlled by the dimerization and weak 2D effects, and the observed optical transitions are the transitions between Hubbard bands.

To some extent, a shift of the maximum of the electronic transition to lower frequencies on cooling can be traced in the spectra of DI-DCNQI₂Ag,¹⁶ but it is much weaker than the tendency observed by us in EDT₂-Br and EDT-AsF₆. While in TMTTF-based salts dimerization within the stacks is well-recognized already at room temperature, in DI-DCNQI₂Ag it develops on cooling thus defining the electronic properties and the position of the optical transition at low temperatures.

A picture in a way similar to ours is presented by solitons in CDW and charge ordered 1D organic conductors, for a review see Ref. 19. An optical band that appears at low temperatures

in spin-Peierls complexes DAP-TCNQ and DAP-DMTCNQ is interpreted in terms of optical response of a soliton.²⁰

V. CONCLUSION

Our optical infrared study of EDT₂-X (X = AsF₆, Br) materials confirms their 1D electronic structure and the stability of charge order with temperature change for EDT₂-AsF₆ material. We probe the infrared optical response of charge carriers in 1D quarter-filled band of EDT₂-X (X = AsF₆, Br) by measuring optical response parallel to the stacks direction (**E** ∥ **a**). We find the optical gap as large as 550 cm⁻¹ for the EDT₂-Br compound and about 700 cm⁻¹ for the EDT₂-AsF₆ material, which is in a good agreement with previous ¹³C NMR studies. In the frequency dependent conductivity spectra in the mid-infrared range (1000-4000 cm⁻¹) we observe an intense band of electronic excitations. The band has an exceptionally strong dependence on temperature, with the spectral weight shifting down in frequencies on cooling. We show that the main reason for this strong dependence is temperature contraction and the respectful change in the transfer integrals *t*. This strong dependence of the position of the mid-infrared electronic transitions on the size of transfer integral *t* suggests the interpretation of the in-stack spectra in terms of domain walls excitations in a 1D Wigner lattice.

ACKNOWLEDGMENTS

We are thankful to A. Jánosy, P. Horsch, and S. Mazumdar for useful discussions. We thank D. Wu and R. Beyer for technical help and for discussions. Á. Antal acknowledges the support of DAAD, T. Knoblauch acknowledges the support of Carl-Zeiss Stiftung, N. Drichko is grateful to Margarete von Wrangell Habilitationstipendium and the American Physical Society for the support.

¹C. Coulon, *J. Phys. IV* **114**, 15 (2004).

²L. Zorina, S. Simonov, C. Mézière, E. Canadell, S. Suh, S. E. Brown, P. Foury-Leykian, P. Fertey, J.-P. Pouget, and P. Batail, *J. Mater. Chem.* **19**, 6980 (2009).

³P. Auban-Senzier, C. R. Pasquier, D. Jerome, S. Suh, S. E. Brown, C. Mézière, and P. Batail, *Phys. Rev. Lett.* **102**, 257001 (2009).

⁴K. Heuzé, M. Fourmigue, P. Batail, C. Coulon, R. Clérac, E. Canadell, P. Auban-Senzier, S. Ravy, and D. Jerome, *Adv. Mater.* **15**, 1251 (2003).

⁵M. Dressel, *Naturwissenschaften* **94**, 527 (2007).

⁶T. Mori, *Chem. Rev.* **104**, 4947 (2004).

⁷M. Mayr and P. Horsch, *Phys. Rev. B* **73**, 195103 (2006).

⁸S. Fratini and G. Rastelli, *Phys. Rev. B* **75**, 195103 (2007).

⁹T. Knoblauch and M. Dressel (unpublished).

¹⁰M. Dressel and N. Drichko, *Chem. Rev.* **104**, 5689 (2004).

¹¹M. Dressel and G. Grüner, *Electrodynamics of Solids* (Cambridge University Press, Cambridge, 2002).

¹²U. Fano, *Phys. Rev.* **124**, 1866 (1961).

¹³A. Damascelli, K. Schulte, D. van der Marel, and A. A. Menovsky, *Phys. Rev. B* **55**, 4863 (1997).

¹⁴K. Yamamoto, A. A. Kowalska, Y. Yue, and K. Yakushi, *Phys. Rev. B* **84**, 064306 (2011).

¹⁵S. Mazumdar and Z. G. Soos, *Phys. Rev. B* **23**, 2810 (1981).

¹⁶K. Yamamoto, T. Yamamoto, K. Yakushi, C. Pecile, and M. Meneghetti, *Phys. Rev. B* **71**, 045118 (2005).

¹⁷N. Drichko, M. Dumm, D. Faltermeier, M. Dressel, J. Merino, and A. Greco, *Phys. C* **460-462**, Part 1, 125 (2007).

¹⁸A. Pashkin, M. Dressel, M. Hanfland, and C. A. Kuntscher, *Phys. Rev. B* **81**, 125109 (2010).

¹⁹S. Brazovskii, *Solid State Sci.* **10**, 1786 (2008).

²⁰T. Sekikawa, H. Okamoto, T. Mitani, T. Inabe, Y. Maruyama, and T. Kobayashi, *Phys. Rev. B* **55**, 4182 (1997).